PERFORMANCE OF A FLAPPED DUCT EXHAUSTING INTO A COMPRESSIBLE EXTERNAL FLOW

P. R. Pratt, J. K. Watterson, E. Benard, S. Hall
School of Aeronautical Engineering, The Queen's University of Belfast
Belfast, BT9 5AG, Northern Ireland

Keywords: *Crossflow, jet, vortices*

Abstract

This paper describes a computational study of the performance of a flapped exhaust duct. The duct curves through 90° so that the exhaust gases are turned into the streamwise direction before passing out into the primary flow. The exhaust port is of rectangular cross-section and a flat plate flap is located on its upstream edge. Mach numbers of 0.4, 0.55, 0.7 and 0.8 are considered and flap angle varied between 15° and 45°; the pressure ratio was varied between 0.64 and 0.97 in order to obtain the range of discharge flow ratio coefficients required. The ratio of boundary layer thickness to orifice length varies between 0.095 and 0.110 and the Reynolds number of the flow at the exhaust leading edge varies between 1.8×10^6 and 3.5×10^6. Thrust and discharge coefficients are predicted. The predictions are validated against published data. The flow is shown to comprise a complex mixture of a jet emerging into a compressible flow, longitudinal vortices generated at the flap side edges, a shear layer shed from the flap trailing edge and, depending on pressure ratio, a normal shockwave. The study will inform a larger investigation into the performance of pressure relief doors.

1 Introduction

It is essential that high pressure systems be protected against damage caused by potential over-pressure. The core engine casing of a bypass turbojet is just one such system; high pressure air is taken off the core compressor for use in a number of auxiliary systems, such as the fan cowl lip skin ice protection system, the turbine cooling system and the cabin air conditioning system. Thus, it is inevitable that the core casing will be transected by ducts carrying pressurized air. Were one of these ducts to burst or develop a leak, the casing would be quickly pressurised and structural damage caused, with the potential loss of the engine. It is necessary, therefore, to install pressure relief doors (PRDs) which will open automatically in response to an over-pressure situation and vent the excess pressure to the fan duct (Fig. 1).

Fig. 1 A typical pressure relief door

In the event of an over-pressure of the engine casing, the pressure difference across the PRD generates sufficient force to open a latch; the door then swings open (it is assumed here that the door is hinged along its leading edge) and quickly assumes a steady angle relative to

the external flow (the maximum deflection would be limited by a lanyard, to protect the external structure from impact damage from the opening door). Once the transient dynamics have settled out, the resultant steady casing pressure is dependent on the discharge flow rate, which is itself dependent on the ratio between the casing and external pressures, the angle at which the PRD settles, the external Mach number and, of course, the size of the opening created. The flow structures formed around such flapped outlets are a complex combination of vortices, an oblique jet and shear layers (Fig. 2; see also Figs. 14-16). The exact combination and development of these structures is dependent on flap angle, free-stream Mach number and pressure ratio.
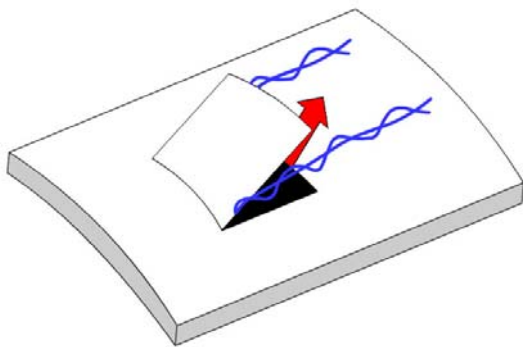

Fig. 2 Longitudinal vortices shed at flap edges

It is necessary that the designer of the PRD system have reliable data on the hinge moment and discharge characteristics. However, the literature on auxiliary intakes is rather old with flapped outlets treated as one of several members of the class (Figs. 3, 4). There are a number of passing mentions of experimental studies specifically related to flapped outlets in papers concerning more generalised auxiliary air systems [1, 2]. Comprehensive experimental data, upon which flapped outlet design might be based, is presented in NACA TN4007 [3] regarding the discharge characteristics of flapped, curved duct outlets in transonic flows. Information on the performance of inclined auxiliary outlets is found in studies by Dewey [4] and Dewey and Vick [5], with these showing

that the discharge performance for given flow conditions is better for outlets with flaps than without.
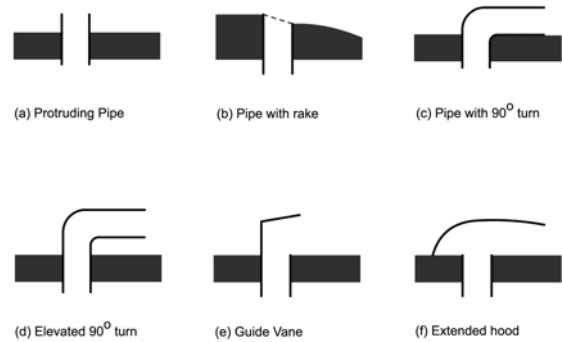

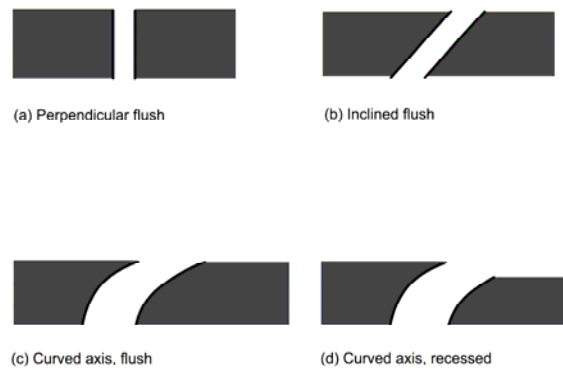Fig. 3 Protruding and hooded outlets

Fig. 4 Flush and recessed outlets

The model geometry described in [3], and chosen for this study, is a flapped outlet which is fed by a rectangular duct; the duct conducts the secondary flow at right angles to the primary flow direction, turning it through a 90° circular arc bend just before the outlet (Fig. 5). Thus, the exhaust flow is pre-conditioned in a manner quite different from that which a core casing flow would experience in an over-pressure event. There is no consideration in [3] of the flow structures formed around or downstream of the outlet and therefore no satisfactory explanation of the effect of flap angle, geometry, pressure ratio or free-stream Mach number on the discharge performance of the outlet.
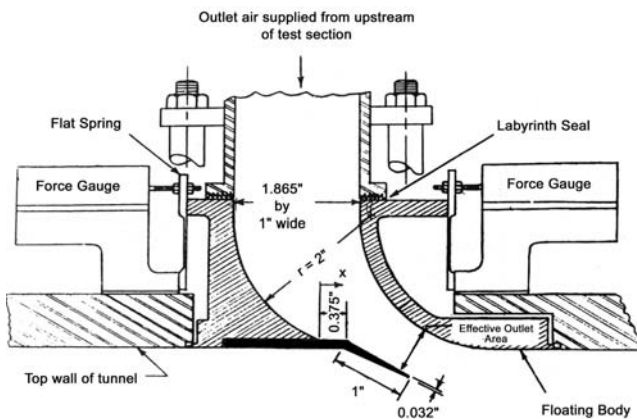
Fig. 5 Flapped outlet geometry adapted from [3]

The purpose of the work described in this paper is to validate the use of a CFD method for the examination of flapped exhaust flows against the data presented in [3]. The flow physics as well as the outlet performance will be examined over a range of Mach numbers, flap angles and pressure ratios. It is the intention of the work then to apply the method to the study of PRDs in which the upstream boundary condition is more representative of that imposed by the core cowl.

2 CFD

2.1 Geometry and mesh

The commercial CFD package, Fluent 6™, was used to model the experimental work described in NACA TN4007 [3]. The computational domain is a rectangular duct 1 inch wide by 1.865 inches in length which turns the exhaust flow through 90° about a radius of curvature of 2 inches into the streamwise direction. The upstream edge of the orifice is extended 0.375 inches so that the orifice length is 1.49 inches. A flat, rectangular flap 1 inch wide by 1 inch long is attached to the upstream edge of the duct orifice. The orifice leading edge was placed 8 inches downstream of the inflow boundary. The computational domain being symmetric, only one half, measuring 17 inches long by 3.125

inches wide by 4.5 inches tall was modelled (Fig. 6).

It was desirable to maintain a structured mesh scheme, where possible, for best capturing boundary layer and shear layer development; but in the region of the flap and the duct exit this proved difficult, where the levels of skew were intolerable. Consequently, an unstructured mesh was fitted to the side face in this restricted area using the Pave function in Gambit™. The Cooper meshing scheme was then used to sweep that face in the *Z*-axis direction.
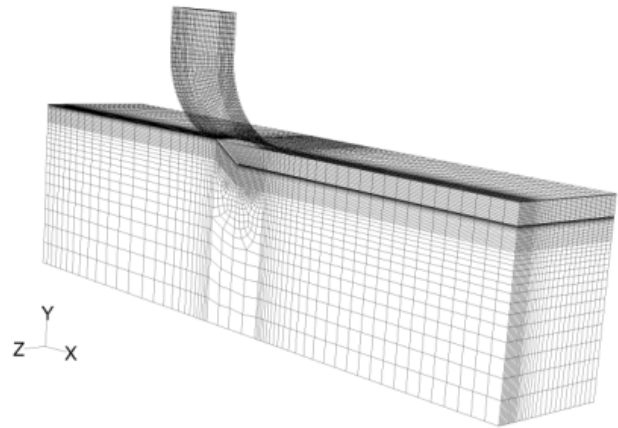
Fig. 6 Model geometry for CFD study

2.2 Equations and boundary conditions

Fluent™ was used in its coupled implicit mode to solve, numerically, the compressible Reynolds-averaged Navier-Stokes equations; SIMPLE pressure-velocity coupling and second order upwind discretisation were employed.

The realisable *k*-ε turbulence model was used because it is of known accuracy when dealing with flows involving jets, separations and secondary flows. Standard wall functions were used to model the influence of the wall. and the value of y^+ for the cell centres adjacent to the wall were set between 30 and 60.

Uniform total pressure and total temperature were specified at the primary inflow boundary; the outflow boundary condition was set as uniform static pressure. The inlet to the exhaust duct was also defined as a pressure inlet, with the total pressure adjusted

to provide the required ratio of internal static pressure to free stream total pressure. The side walls of the computational domain and the wall opposite the exhaust duct were defined as symmetry planes.

2.3 Flow conditions and post-processing

Flap angles of 15° to 45°, in 5° increments, were studied. The free stream Mach number was varied from 0.4 to 0.85 in increments of 0.15. As a result, the ratio of boundary layer thickness to orifice length varied between 0.095 and 0.110. The pressure ratio was varied between 0.64 and 0.97 in order to obtain the range of discharge flow ratio coefficients (DFR) required. In this context, DFR is defined as

$$DFR = \frac{\dot{m}}{\rho V_\infty A} \qquad (1)$$

where $\dot{m}$ is the mass flow rate through the outlet; the terms in the denominator refer to free stream conditions and A is the effective outlet area, determined by the distance between the flap and the opposite wall of the curved outlet duct (Fig. 5). Mass flow through the effective outlet area was calculated from the data files and DFR was calculated for each case, doubled to account for the symmetry plane. The force on the flap, and the load centre were extracted and used to calculate the moment about the hinge line for each case. This was converted to pitching moment coefficient by normalising with respect to the free-stream dynamic head, effective outlet area and flap length, with positive moment defined to be closing the flap.

2.4 Mesh dependence study

A mesh dependence study was performed to ensure that converged solutions were mesh independent. For one case, three meshes with approximately 58,000, 150,000 and 270,000 cells, respectively, were created. The streamwise distribution of pressure coefficient along the centreline (Fig. 7) suggest that the solution on the coarsest mesh is sufficiently well resolved. However, Fig. 8 shows the distribution

of total pressure through the core of the vortex that streams off the side edge of the flap; the total pressure deficit in the core is only resolved by the two finer meshes. Consequently, all subsequent calculations were performed with meshes containing about 160,000 cells.
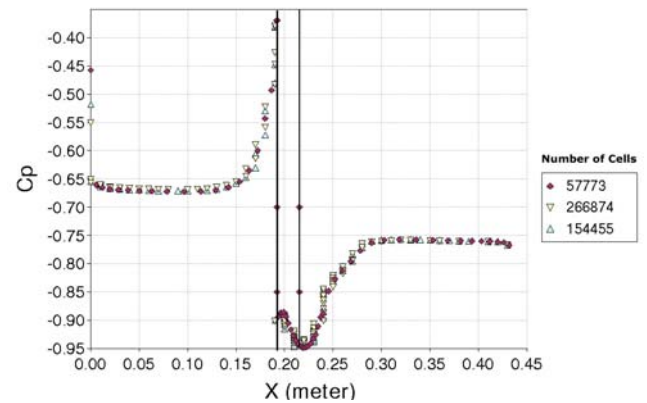

Fig. 7 Streamwise distribution of pressure coefficient on the centreline for three mesh densities
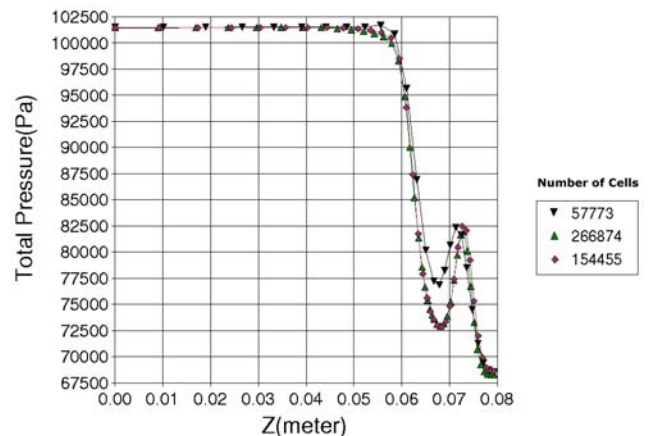

Fig. 8 Total pressure through the core of the flap vortex for three mesh densities

3 Results and Discussion

3.1 Outlet performance

To investigate the accuracy and validity of the CFD model, DFR and pressure ratio data were extracted from the numerical predictions for a single flap angle and plotted in Fig. 9 with the corresponding data from [3] for a range of Mach numbers. Fig. 9 indicates that the experiments covered a wider range of DFR than the CFD;

this was simply because the modelling exercise was but one step in a larger programme of research, and it was unnecessary to cover the whole range of conditions. It should also be appreciated that the adjustment of the total pressure boundary condition on the exhaust duct inlet to achieve the desired DFR was not pursued to the nth degree.

The curves through the predicted data points match the trend of the curves for the experimental data. However for a given pressure ratio the CFD result appears to under predict the DFR. This discrepancy increases with increasing pressure ratio with the effect becoming more severe with increasing free-stream Mach number. The maximum error at each Mach number increases from 5% at M=0.4 to 20% at M=0.85.

The thrust generated by the outlet, defined positive in the stream-wise direction, was measured in the NACA paper through the use of a force gauge (Fig. 5) and non-dimensionalised with free stream dynamic head and effective outlet area. For comparison, the same thrust coefficient was calculated using the CFD results, taking into account the force on both the curved duct and flap. The envelope of thrust data from the NACA experiments is plotted in Fig. 10, along with the corresponding CFD data points, for a single flap angle. At lower values of DFR the predicted values of thrust fall within the envelope from the experimental data. At the larger values of DFR the CFD results over-predict the generated thrust with the points lying just outside the envelope, with an error between 5% and 10%.

DFR is plotted in Fig. 11 against angle for each pressure ratio and Mach number. In each case DFR increases with flap angle up to a maximum before falling off. The angle at which this maximum occurs decreases with increasing pressure ratio. Increasing Mach number also reduces the angle at which maximum discharge occurs. The maximum value of DFR increases with increasing pressure ratio but decreases with increasing Mach number.

Flap hinge moment coefficient is plotted against flap angle in Fig. 12. The moment coefficient increases with increasing Mach

number, pressure ratio and flap angle, above flap angles of 25°. Extrapolation of the data shows that for the majority of combinations of pressure ratio and Mach number, the zero pitching moment coefficients occurred in the range of 10° to 15°. At lower pressure ratios and Mach numbers this point is lowered below 10°.
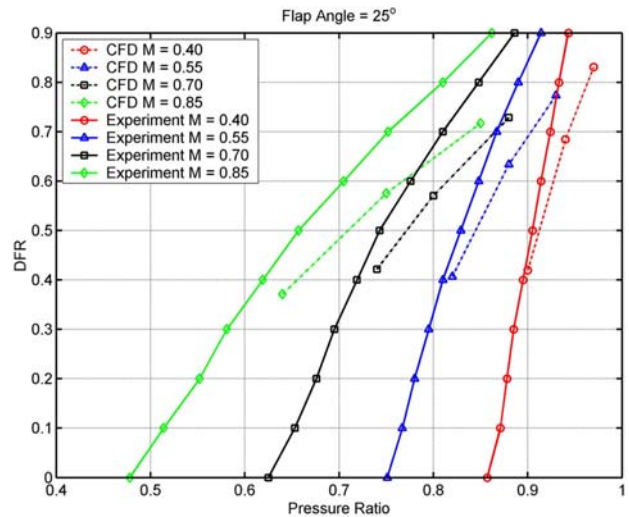

Fig. 9 DFR against pressure ratio, for flap angle=25°, comparing NACA TN4007 and CFD results
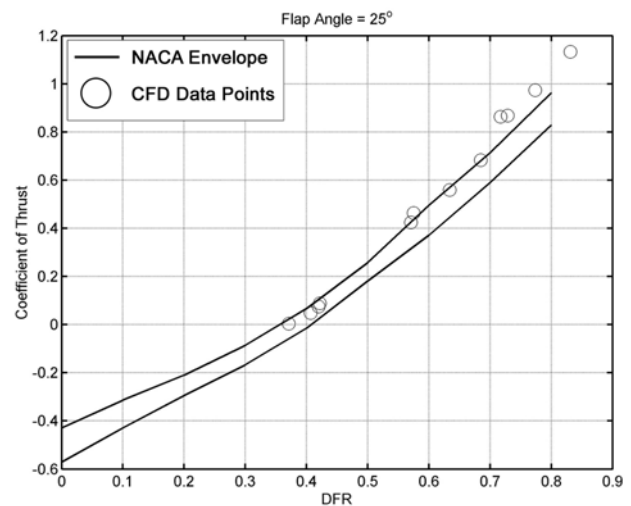

Fig. 10 Coefficient of thrust against DFR, for flap angle=25°, comparing NACA TN4007 and CFD results

For completeness, predicted thrust coefficients are shown in Fig. 13. It appears that thrust is strongly dependent on the DFR or pressure ratio. As flap angle increases, the vortices generated at the flap edges strengthen and thrust drops in a non-linear manner.
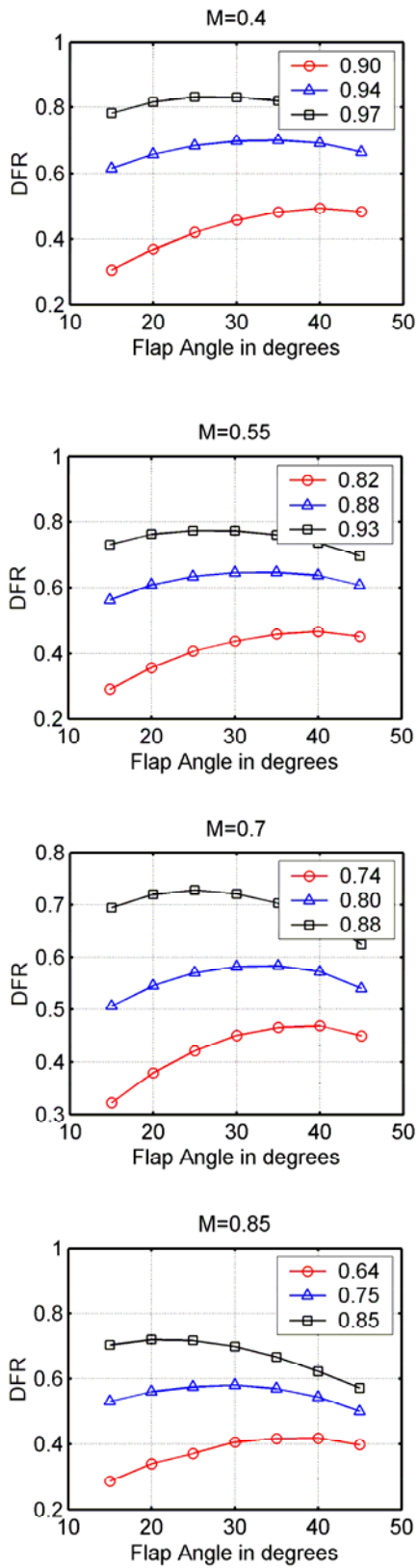
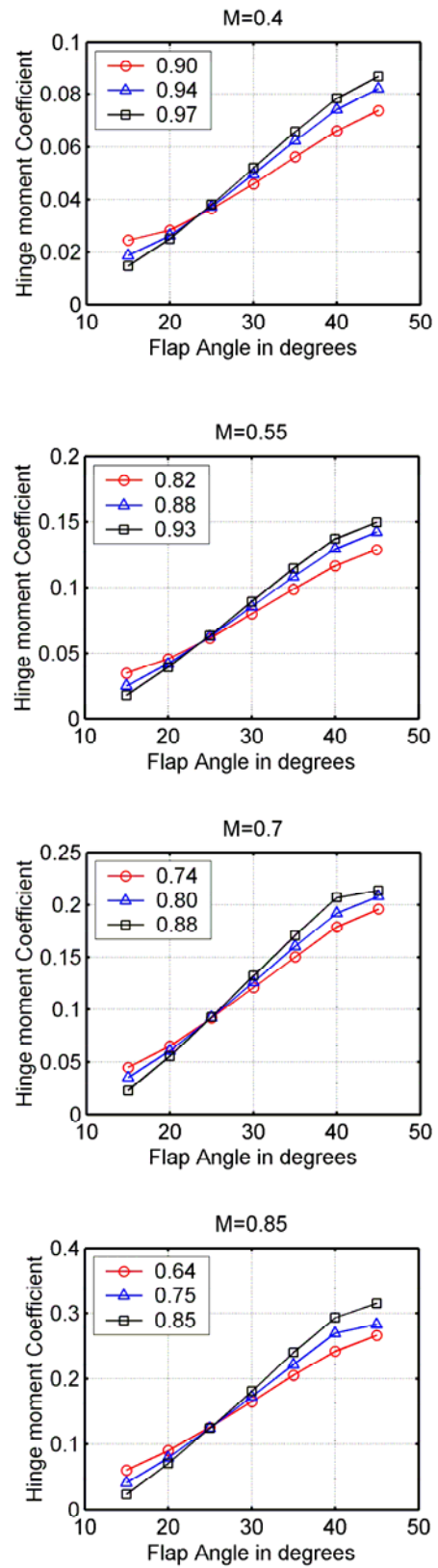Fig. 11 DFR against flap angle for a range of pressure ratios and angles

Fig. 12 Hinge moment coefficient against flap angle for a range of pressure ratios and Mach numbers
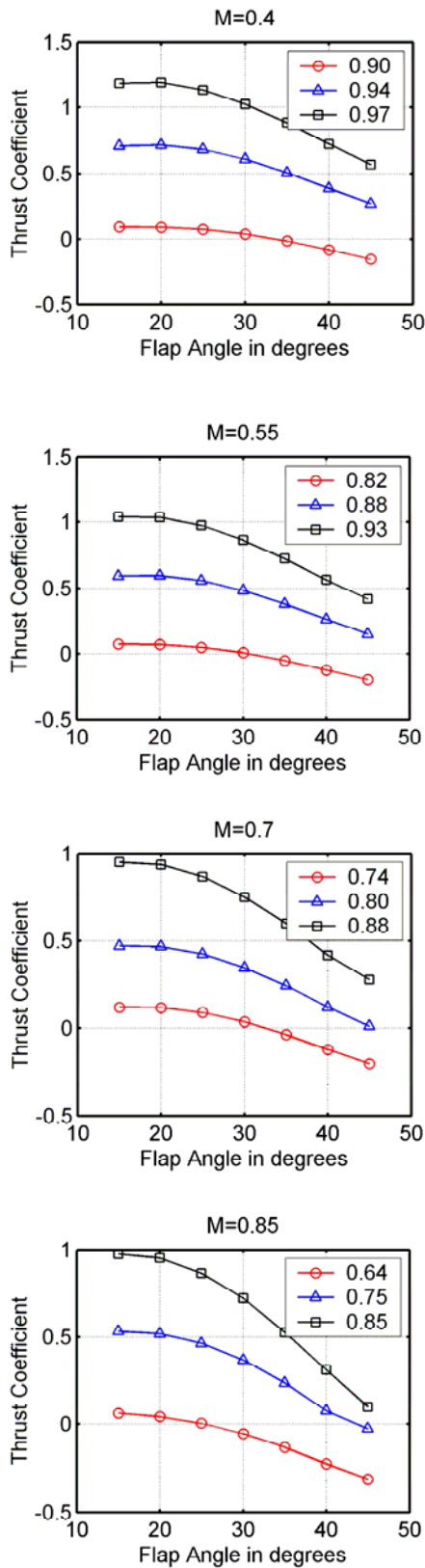
Fig. 13 Thrust coefficient against flap angle for a range of pressure ratios and angles

3.2 Outlet aerodynamics

From the plots in Fig. 11 it can be seen that flap angle has a pronounced effect on the discharge performance of the outlet. Previous studies [1, 2] had indicated that flaps, or other protrusions, generated areas of low pressure over the outlet which increased discharge through suction. The mechanism behind this is the formation of a pair of longitudinal vortices, shed from the edges of the flap (c.f. the leading edge flow on a delta wing). As the flap angle increases, the strength of the vortices increases until a maximum angle is reached. Beyond that angle the flap could be said to "stall" and behaves like a bluff body.

Fig. 14 shows a series of plots of total pressure contours in Y-Z planes of the computational domain, downstream of the outlet, for a flap angle of 15°, free-stream Mach number of 0.7 and pressure ratio of 0.8. Note that the symmetry plane has been plotted to illustrate the vortex pair of generated at the flap edges. The structure of the flow can be seen to develop downstream of the outlet as the vortices interact with the exhaust jet and shear layer shed from the trailing edge of the flap.

Fig. 15 shows a similar plot for a flap angle of 40° but with the same pressure ratio and free-stream Mach number, as shown in Fig. 14. A marked difference in the flow field can be seen, with a much stronger initial vortex pair leading to a larger flow structure further downstream. For the smaller flap angle, the flow structure impinges on the surface downstream which appears to have a thinning effect on the boundary layer in the downstream area outboard of the vortices. Fig. 15 however shows that for a large flap angle the structure is lifted away from the surface with the result that the boundary layer thinning does not occur; in fact, between the vortices the boundary layer is substantially thickened.

It is this non-linear behaviour of the development of the flap edge vortices that is responsible for the non-linearity of the results presented in Figs. 11 to 13. In particular, the lower pressure imposed by the vortex pair on the duct outlet may be expected to be an important factor in the DFR. A failure to model

correctly the interaction between the exhaust flow and the vortex generation mechanism may, therefore, explain in part the under-prediction of DFR for various Mach numbers and pressure ratios presented in Fig. 9.
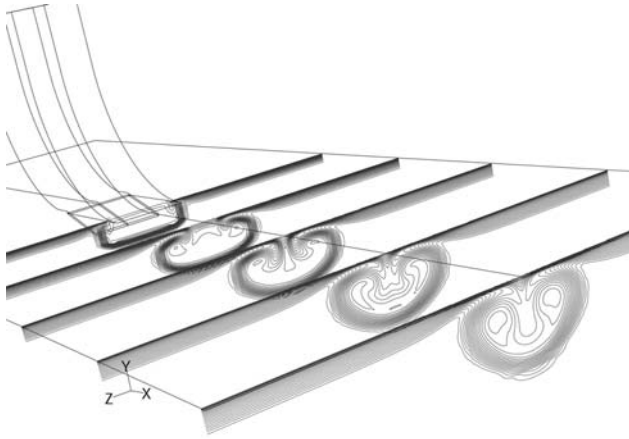

Fig. 14 Contours of total pressure, flap angle = 15°, M=0.7, pressure ratio = 0.8
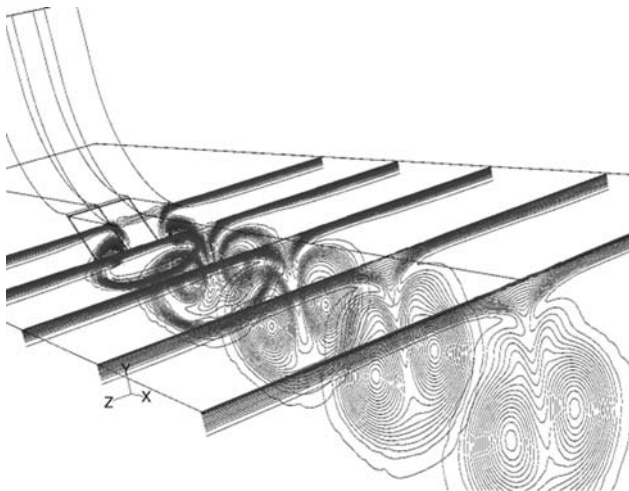

Fig. 15 Contours of total pressure, flap angle = 40°, M=0.7, pressure ratio = 0.8

Variations in pressure ratio will change the nature of the discharge jet from the outlet, which will then in turn effect the manner in which the vortices, jet and shear layer interact. Free stream Mach number will also determine the properties of the shed vortices and the resulting flow structure. In cases of high Mach number and pressure ratio, flow in the outlet becomes choked as flow velocity exceeds sonic conditions and a normal shock is formed, as

illustrated in Fig. 16. The position of this shock moves forward as the flap angle decreases, due to a repositioning of the throat of the outlet as effective area decreases.
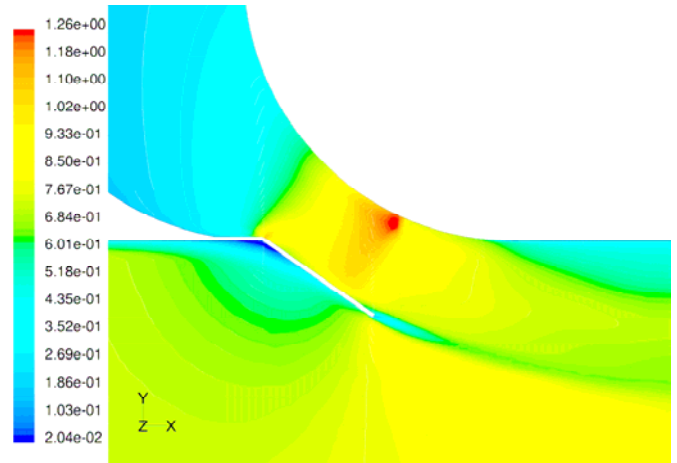

Fig. 16 Contours of Mach number, flap angle = 35°, free-stream M=0.85, pressure ratio = 0.85

4 Conclusions

Generally good agreement was obtained between measurement and prediction of integral quantities such as DFR and thrust coefficient. Predictions under estimated DFR by between 5% and 20%, depending on pressure ratio; the thrust coefficient was slightly over-predicted.

Calculations were performed for a wider range of flap angles than was considered in the experiments, and it was shown that the DFR increases with flap angle up to an optimum value, after which increasing flap angle decreases the DFR. The value of optimum angle falls with increasing pressure ratio, but rises with increasing free stream Mach number. These effects may be explained, in part, by the strength and orientation of the vortex system generated by the inclined flap, which sets a boundary condition on the flow emerging from the exhaust duct.

It was shown that the angle for which the pitching moment on the flap was zero lay in the range of 10° to 15° for all cases. A freely hinged, weightless flap would, therefore, achieved a trimmed balance in that range of angles. Increasing Mach number decreases this

angle, while increasing pressure ratio increases it.

References

[1] Rogallo F M. Internal-flow systems for aircraft. NACA Report 713, 1941.

[2] Drag of Auxiliary Inlets and Outlets. AGARD, 264.

[3] Vick A R. An Investigation of Discharge and Thrust Characteristics of Flapped Outlets for Stream Mach Numbers from 0.4 to 1.3. NACA TN 4007, 1957.

[4] Dewey P. A Preliminary Investigation of Aerodynamic Characteristics of Small Inclined Air Outlets at Transonic Mach Numbers. NACA TN 3442, 1955.

[5] Dewey P and Vick A R. An Investigation of the Discharge and Drag Characteristics of Auxiliary Air Outlets Discharging into a Transonic Stream. NACA TN 3466, 1955.